DOI: 10.24352/UB.OVGU-2018-033 TECHNISCHE MECHANIK, 38, 3, (2018), 256 - 266
submitted: June 27, 2018

Assessment of Various Diffuser Structures to Improve the Power Production of a Wind Turbine Rotor

Yiyin Klistafani[1,*], M. Iqbal Mukhsen[1], and Galih Bangga[2,3,†]

Numerical simulations were carried out for the flow field around various diffuser type structures to improve the performance of a small wind turbine rotor. The present studies specifically investigate the effect of four different shapes of diffuser, namely flat diffuser, curved diffuser, flat diffuser with inlet shroud, and curved diffuser with inlet shroud on the wind velocity characteristics. Numerical studies were conducted using the Computational Fluid Dynamics (CFD) method. A reasonable agreement between the computed results and available experimental data is obtained. The studies demonstrate that the curved diffuser generates the strongest increment of the wind velocity compared to the other configurations.

Keywords: CFD, DAWT, Diffuser, Wind energy, Wind turbine

1 Introduction

An increasing demand for energy is not comparable with the availability of fossil fuel. Therefore, efforts to develop alternative energy utilization should be encouraged. Wind is one of the renewable energy resources which is clean and sustainable. Wind power investigation is very important to address environmental issues, such as global warming and air pollution. It is well known that wind speed fluctuates, and accordingly its energy potential, depending on the nature of climates. One of the inhibiting factors in the utilization of wind energy conversion technology is that the wind speed is often too low for the application of wind power extractor. It is well known that wind turbines usually operate for the rated wind speed of around 8-11 m/s (Bangga et al, 2017a,b). The power of the wind is proportional to the cubic power of the wind velocity approaching a wind turbine. This means that even a small amount of its acceleration gives large increase on the energy generation (Abe and Ohya, 2004). Therefore, wind turbine innovation is required in optimizing the utilization of wind energy, especially in areas with low wind speed potential. One of the developing concepts is the engineering design of diffuser type structure for the development of DAWT (Diffuser Augmented Wind Turbine).

Selection of the diffuser type structure as a good shroud for wind turbine was given by Ohya et al. (2008) who employed three typical hollow structures, namely nozzle type, cylinder type, and diffuser type. It was confirmed that the diffuser structure was the most effective for collecting and accelerating the wind than other hollow structures. Based on the results, they did further examination on four developed diffuser type structures, namely diffuser only, diffuser with inlet shroud, diffuser with flange, and diffuser with inlet shroud and flange. It was found that the wind speed was increased by adding an inlet shroud and a ring-type flange at the exit periphery to the diffuser body (Ohya et al, 2008). Purwanto and Nasution (2010) modified diffuser interior in order to optimize performance of DAWT. They found that modifying diffuser interior into curved shape could increase the maximum wind speed up to 30%.

With the development of computer technology, it is possible to model engineering problems using Computational Fluid Dynamics (CFD) approaches. Different types of simulations have been compared and validated against measurement data since then. The simulations range from the simplest 2D Reynolds-Averaged Navier-Stokes (RANS) approach to the most complex Direct Numerical Simulation (DNS) approach. However, the latter is not possible to be carried out for the complex structure for the time being due to its large computational effort, because all the turbulent structures are resolved. Wang et al. (2010) investigated the dynamic stall behaviour of a pitching airfoil in comparison to the experimental data using the Shear-Stress-Transport (SST) k-ω (Menter, 1994) and Wilcox k-ω (Wilcox, 1993) turbulence model. They concluded that the Wilcox (or standard) k-ω model was too dissipative and could not deliver the prediction accurately. On the other hand, the SST model provided a better agreement against the experimental data. Bangga and Sasongko (2017) attempted to further improve the prediction accuracy by modifying the turbulent viscosity near the wall where flow separation and the shear stress is the strongest. The modification involves a damping factor where the turbulence is reduced to a certain value locally within the buffer layer. The standard k-ε model according to

Launder and Spalding (1972) was tested for this purpose. The results were compared against four most employed turbulence models, namely the standard k-ε, realizable k-ε, Wilcox k-ω, and SST k-ω models, and available experimental data. The results indicated that the modified model, SST k-ω model and realizable k-ε model provided the most accurate prediction for the flow associated with strong separation. A similar improvement was also obtained when the idea was implemented for the SST k-ω model incorporating a separation detection mechanism by means of the ratio of the turbulent kinetic energy to its specific dissipation rate (Bangga et al, 2018). A good agreement of the CFD computations using the SST turbulence model was also obtained in several computations, for example Pape and Lecanu (2004). Sørensen et al (2002), Bangga et al (2017c,d), Bangga (2018), Weihing et al (2016), and Jost et al (2017). These encourage the use of CFD for predicting the fluids engineering problems especially with the help of the Menter SST k-ω model. Having considered the above background, the development of a wind power system with high output aims at determining how to collect wind velocity efficiently and what kind of diffuser design can generate energy effectively from the wind speed. In the present studies, several numerical investigations will be carried out for the flow field around diffuser structures aiming to identify the optimized configuration. The computed results will be compared against available experimental data to show the fundamental capability of the model for predicting complex turbulent flows. The paper is organized as follow. Section 2 presents the numerical setup, Section 3 presents the validation and discussion of the results. Section 4 provides the annual energy potential analysis based on the outcome of the present studies, and all of them will be concluded in Section 4.

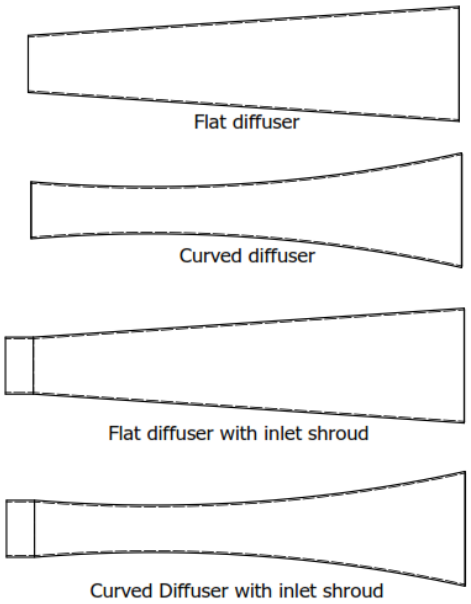

Figure 1. Diffuser type structure designs.

2 Numerical Methods and Validation

In the present section, the detailed description of the employed methods is given. The CFD studies mainly concern about the flow development around four types of diffuser. A steady two-dimensional approach was employed for the present studies. It will be shown that this is sufficient for predicting the main flow features, but not the wake behaviour of the flow. However, the latter is not of interest as the focus of the present studies is only for estimating the flow acceleration inside the diffuser. The geometry was created using Ansys Workbench. The flat diffuser was generated according to the geometry specified in the experimental studies carried out by Ohya et al (2008). The design of the curved shaped diffuser was adjusted based on the flat diffuser dimensions by specifying the curvature. The diffuser has a thickness of 1.25 cm. This was designed based on the recent studies by Hu and Wang (2015) who employed ten layers of plate with each has a thickness of 1.25 mm. Four different types of diffuser were introduced, namely the flat diffuser, curved diffuser, flat diffuser with inlet shroud, and curved diffuser with inlet shroud. These structures are illustrated in figure 1. Detailed information about their dimension is given in table 1 and figure 2.

Table 1. Diffuser type structure (2D) dimensions

Specification	Diffuser Type Structure			
	Flat diffuser	Curved diffuser	Flat diffuser with inlet shroud	Curved diffuser with inlet shroud
Inlet diameter (*D*)	40 cm	40 cm	40 cm	40 cm
Diffuser Length (*L*)	308 cm	308 cm	308 cm	308 cm
Diffusser thickness (*t*)	1.25 cm	1.25 cm	1.25 cm	1.25 cm
Inlet shroud length (*l*)	-	-	20 cm	20 cm
Diverging angle (α)	4^o	4^o	4^o	4^o
Circle radius of arch (r)	-	1000 cm	-	1000 cm

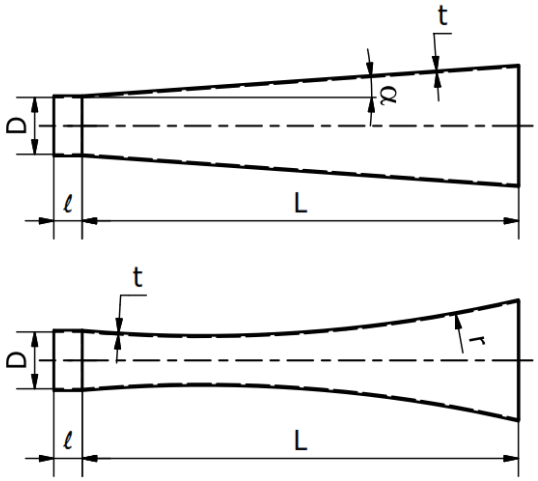

Figure 2. Detailed dimensions of the flat diffuser with inlet shroud and the curved diffuser with inlet shroud.

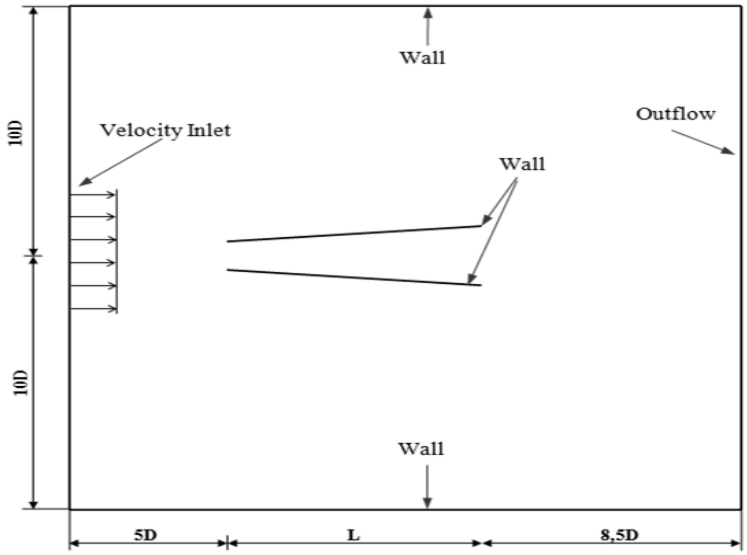

Figure 3. Computational domain and its associated boundary conditions of the flat diffuser.

Table 2. Mesh parameters and controls of flat diffuser

Mesh Parameters		Mesh Controls	
Size function	Curvature	Method	Quadrilateral dominant
Relevance center	Fine	Free Face Mesh Type	All Quad
Max. skewness	0.9	Bias factor	5
Smoothing	High		
Inflation Option	Smooth transition		
Transition Ratio	0.272		
Growth Rate	1.2		
Maximum layers	2		
Minimum Edge Length	1.25e-002 m		
Nodes	67931 (Grid 2)		
Elements	66836 (Grid 2)		

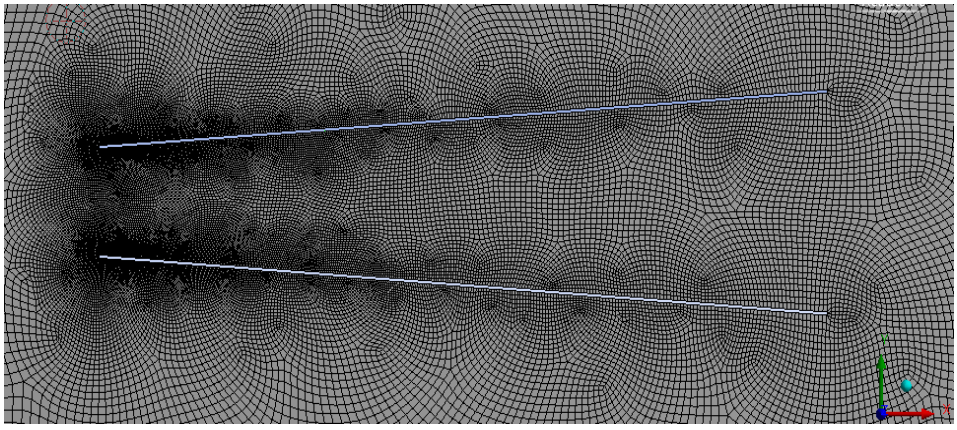

Figure 4. Zoom of the mesh near the flat diffuser wall

The domain of the simulation is illustrated in figure 3. The inlet of the flow is located at 5 times the inlet diameter of the diffuser (D). The velocity inlet boundary condition was applied at this location. The flow leaves the computational domain at 8.5D distance from the outlet plane of the diffuser with the outflow boundary condition. The side walls were set as a non-slip wall that are sufficiently far away from the area of interest to ensure the minimal effect on the flow characteristics near the diffuser. The present studies assume the case to be a plain stress problem instead of a rotationally symmetric problem that usually applies for the case where the cross section is circular. This is done in order to make the analyses hold also for the case where the cross section is square. The square diffuser is usually useful for vertical axis wind turbines. Furthermore, the comparison with the experimental data in figure 5 verifies that the chosen boundary condition is still acceptable even for the circular cross section case. The present studies analyze the flow in the axial and lateral axes. In this sense, the gravity can be neglected in the computations. The computations were carried out using the commercial software Ansys Fluent 18.2. The flow was assumed to be steady and the incompressibility effect was neglected. This is reasonable because wind turbines usually operate at a much smaller velocity than the speed of sound. An initial undisturbed wind velocity of 5 m/s was prescribed at the velocity inlet plane. The same velocity was employed by Ohya et al (2008) in their experiment. The turbulence closure was modelled using the two-equation SST k-ω model according to Menter (1994). This model combines the standard k-ε model (Launder and Spalding, 1972) in the freestream and the Wilcox k-ω model (Wilcox, 1993) for the wall bounded flow. The model is good for predicting flows with a strong adverse pressure gradient as demonstrated already in Hu and Wang (2015); Bangga and Sasongko (2017), Bangga et al. (2018), Pape and Lecanu (2004), Sørensen et al (2002), Bangga et al (2017c,d), Weihing et al (2016), and Jost et al (2017). The pressure velocity coupling uses the SIMPLE method. All the variables were solved using the second order discretization. The computations were carried out for 10,000 iterations, otherwise convergence was achieved if the residual of the momentum reaches 1e-6.

The mesh was generated using ANSYS Workbench 18.2 software. Mesh parameters and controls are shown in table 2. An enlarged view of the mesh near the flat diffuser wall is shown in figure 4. Grid independence studies were carried out in advance to ensure that the results are independent of the mesh resolution. The results are plotted in Figure 5 where the streamwise velocity ratios (U/U_∞) of the six meshes are compared. It can be seen that grid 2 has good agreement to experimental results with a relative error of about 6.01%.

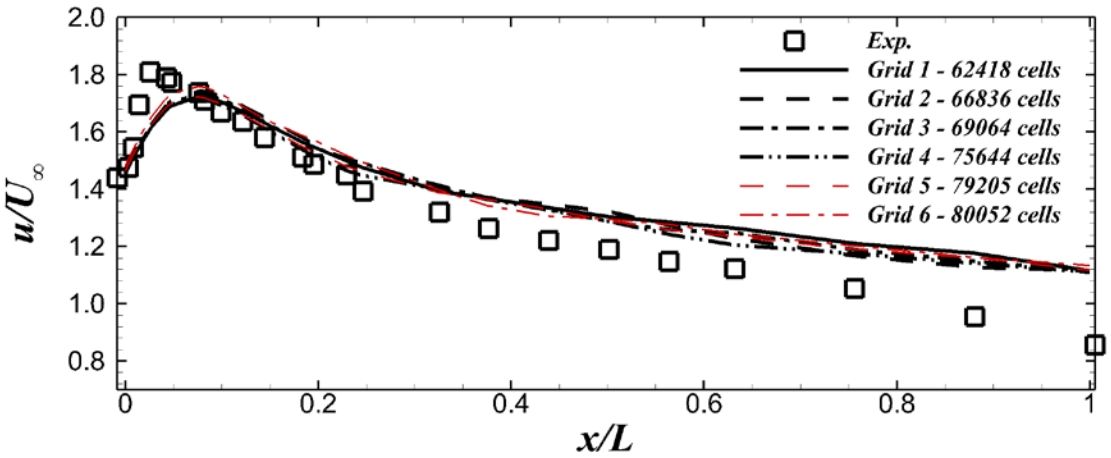

Figure 5. Grid Independence - streamwise flow velocity distribution for the flat diffuser at the centreline.

For a further validation, not only quantitative comparison is shown, but also the qualitative comparison is presented. The turbulence kinetic energy contour is compared with the flow visualization by Ohya et al. (2008) as shown in figure 6. The smoke-wire technique was employed for the flow visualization experiment. As seen in figure 6, the wind flows into the diffuser as it is inhaled. Turbulence kinetic energy contour in the simulation shows similarities with visualization experiment.

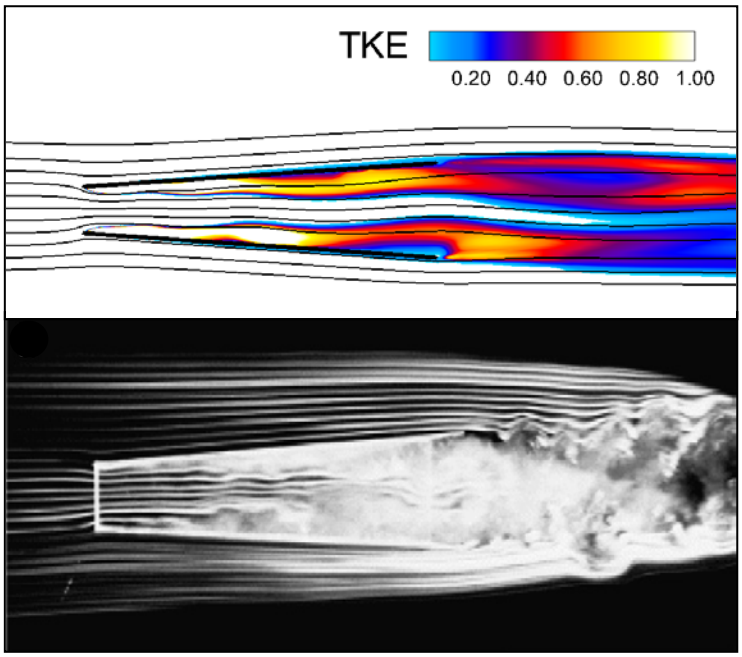

Figure 6. Qualitative comparison between numerical and experimental results: turbulence kinetic energy in m^2/s^2 (top) and smoke flows (bottom).

3 Results and Discussion

The dimensionless streamwise velocity U/U_∞ at midline diffuser plots for four diffuser type structures are presented in figure 7. The distribution of the axial velocity (U) is chosen in the present studies instead of the lateral velocity (V) because the corresponding wind speed is more dominant and determines the power generated by the turbine. In case of the diffuser type structures, the distribution of the axial velocity reveals that the maximum velocity occurs for curved diffuser. It is found that the inlet shroud has no significant impact on the augmentation of the wind velocity; otherwise it generates some negative impact. The difference in increased velocity generated by the curved diffuser compared to flat diffuser is 5.74%. The curved diffuser shows a better performance. However, the maximum velocity occurs at the different sections (x/L) between flat diffuser and curved diffuser. A closer look into the velocity at the entrance section (x/L = 0) shows that the flat diffuser with inlet shroud actually generates a higher velocity at the entrance section. It is noted, however, that the curved diffuser has a better performance than the flat diffuser, provided that location of the rotor is not at the near entrance but around $x/L \approx 0.36$. Detailed information regarding the comparison of the wind velocity at midline of all diffuser type structures is shown in table 3.

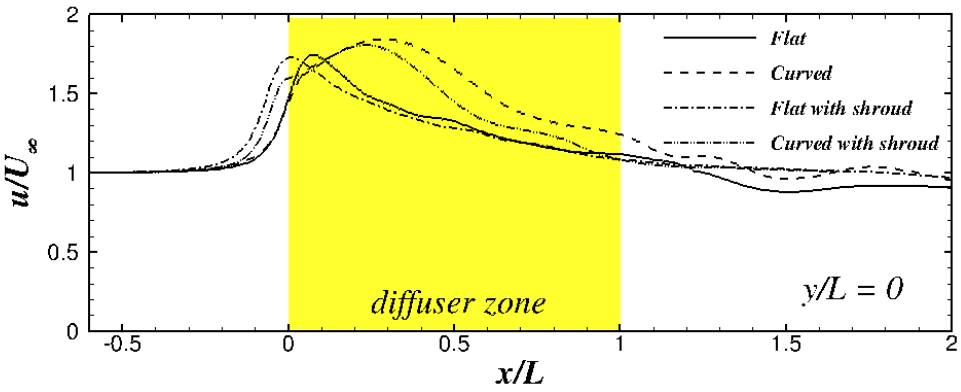

Figure 7. Wind velocity distributions at the midline axis along the axial positions for four different diffuser types.

Table 3. Wind velocity at midline for all diffuser type structures

Value	Flat diffuser	Curved Diffuser	Flat diffuser with inlet shroud	Curved diffuser with inlet shroud
Wind velocity at entrance, x/L = 0 (m/s)	7.34	7.20	8.63	7.98
Maximum wind velocity (m/s)	8.71	9.21	8.64	9.02
Increment	74.23%	84.18%	72.80%	80.39%

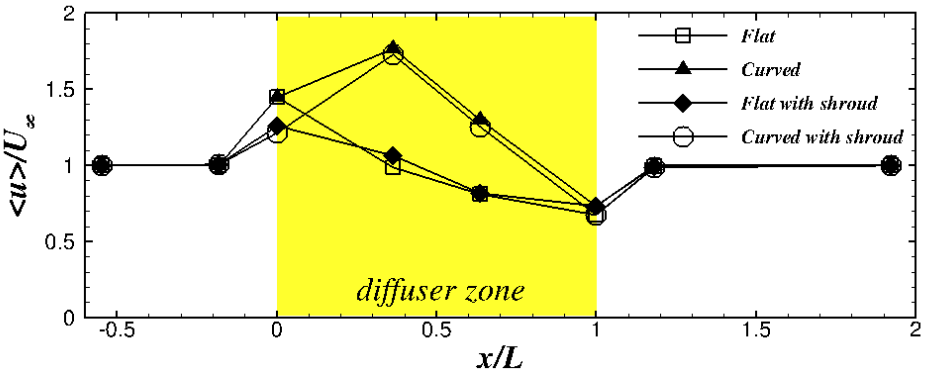

Figure 8. Average wind velocity distributions along the axial positions for four different diffuser types.

Further comparison of the dimensionless streamwise velocity U/U_∞ for four diffuser type structures are presented in figure 8, in which the average velocity data are taken at each section of diffuser. As shown in figure 8, the wind velocities for four diffusers are similar upstream of the inlet diffuser zone. Diffusers equipped with the inlet shroud have the smaller average wind velocity at the entrance (inlet diffuser, section x/L = 0) than diffusers without the shroud (section x/L = 0). This fact is in contrary to the preceding explanation given in figure 7 and table 3. Note that these increased velocity of the diffuser equipped with the shroud actually occurs in the centreline of the diffuser (entrance section, x/L = *0*). It shows that the actual wind velocity at the midline diffuser is not capable of representing the overall velocity of each section. Figure 8 shows that the average wind velocity at the diffuser zone for the curved diffuser is higher than the flat diffuser. However, in the diffuser outlet, the average wind velocities of four diffusers have no significant difference to the downstream zone. The highest value of the averaged maximum wind velocity of 76.99% ($u/U\infty$ = 1.77) is produced by curved diffuser.

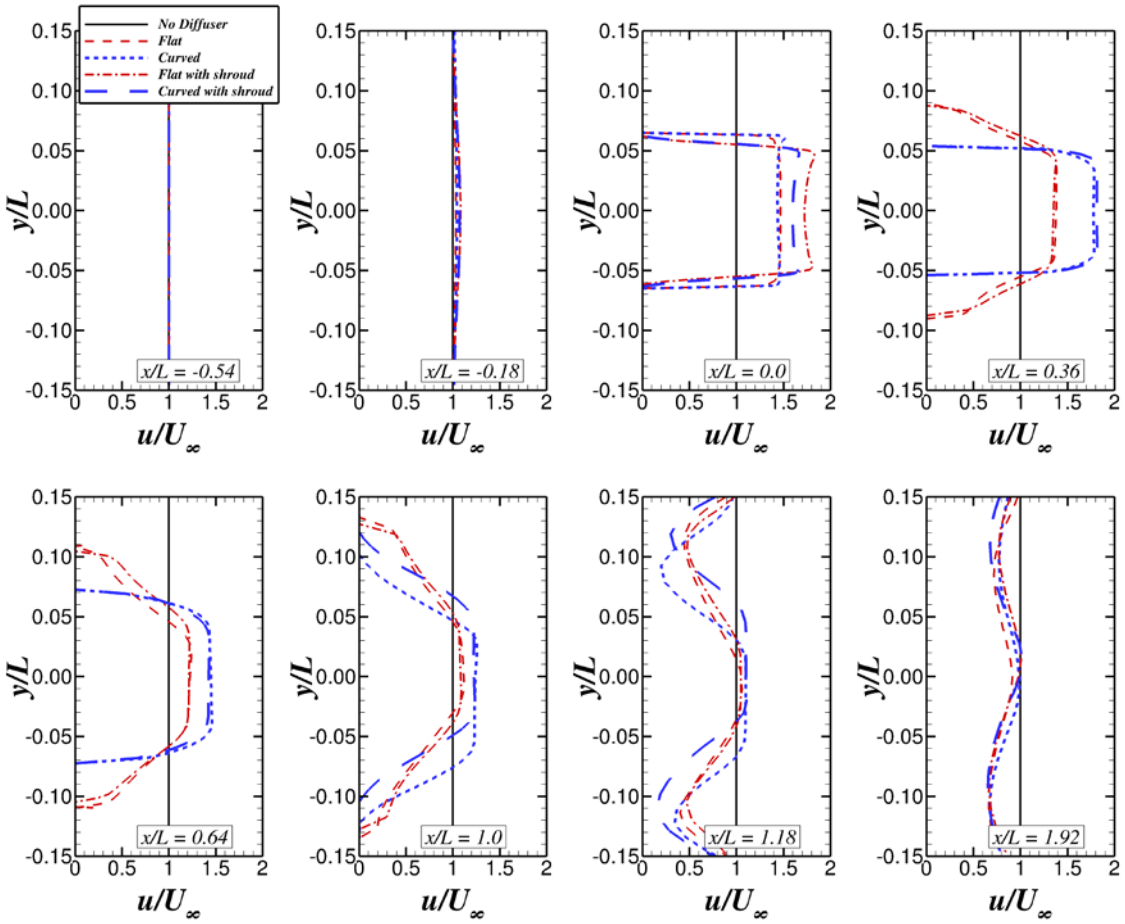

Figure 9. Velocity profiles for four different diffuser types along *y*-coordinate at several axial positions.

To clarify the rate of wind flow within and without diffuser, figure 9 presents the velocity profile for the four investigated diffusers. It can be seen that the wind velocity at the upstream zone (far away from inlet diffuser, x/L = -0.54) is not influenced by the presence of the diffuser. It becomes evident that the wind velocity slightly increases at the near inlet diffuser (x/L = -0.18). The increase in wind velocity is very visible at the entrance diffuser (x/L = 0), where the flat diffuser equipped with the inlet shroud has the best performance than the others. However, the greatest increase in wind velocity along the diffuser (x/L = 0.36 until x/L = 1) is actually generated by the curved diffuser. Overall, it can be clearly seen that the wind velocity is much higher in all diffuser types than the case without the diffuser. The increment of the wind velocity is not shown at downstream zone (far away from outlet diffuser, x/L = 1.92). In fact, the wake flow occurs within this area that can cause a problem if the other turbines are designed to operate within the downstream area.

Figure 10 shows the comparison of the flow energy production for four diffuser types and a case without diffuser. The difference in the flow energy production between flows through the diffusers and without diffuser is evident in the section x/L = 0. Flat diffuser with inlet shroud can produce the highest increment of flow energy

production only at inlet diffuser (x/L = 0), while curved diffuser can produce the best increment of flow energy production through the diffuser. These correspond to velocity profile in figure 9 where the higher the increment of the wind velocity the higher the flow energy production.

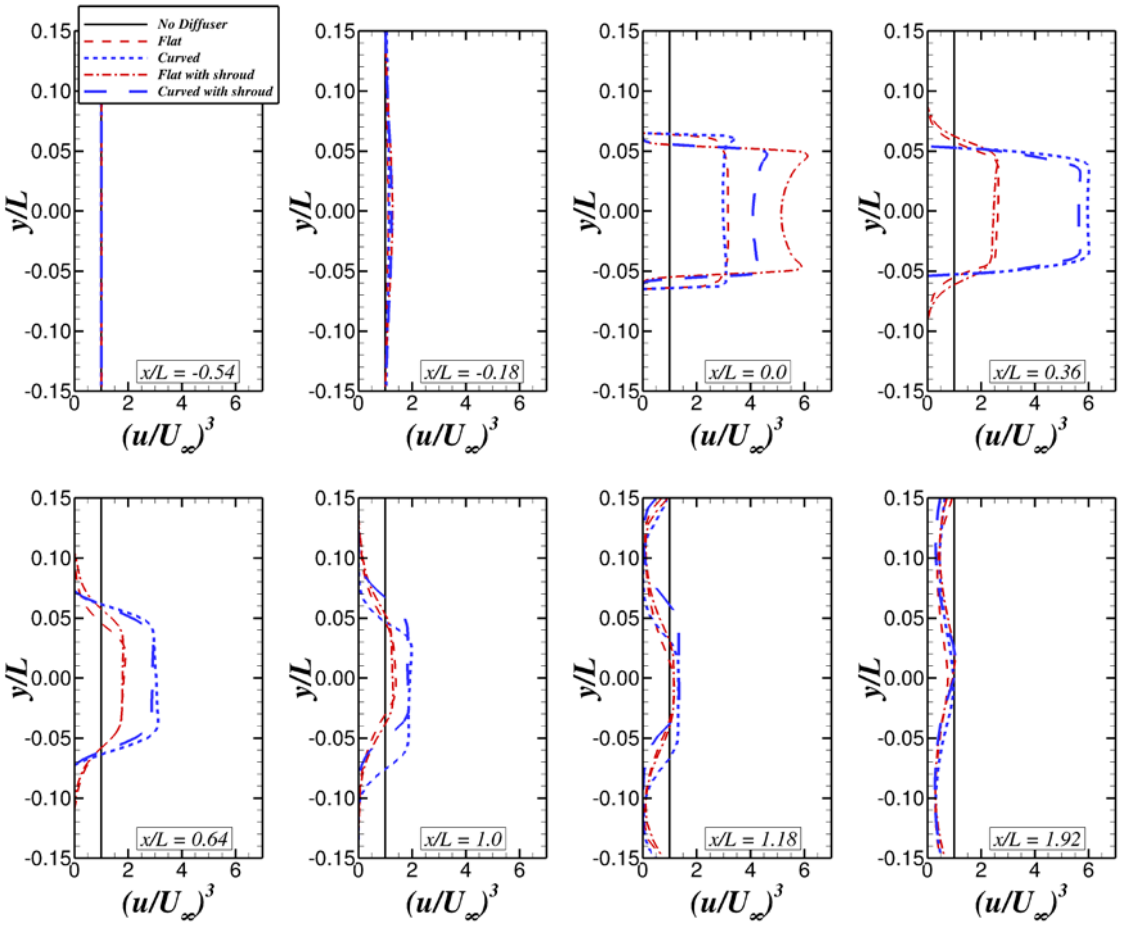

Figure 10. Flow energy profiles for four different diffuser types along *y*-coordinate at several axial positions.

To estimate the generated power production of the turbine equipped with the diffuser, the research vertical axis wind turbine (VAWT) investigated by Saedi et al (2013) is considered. The turbine has a radius of 2 m and a height of 1.38 m. The estimated power curves of the turbine for various wind speeds and diffusers are shown in figure 11. In these plots the turbine is assumed to be located at x/L = 0.36 where the maximum average wind speed (v) takes place. It can be seen clearly that the diffuser increases significantly the power generated by the turbine especially at a higher wind speed case. The analysis can be further enhanced by considering the Weibull distribution of the wind speed as:

$$f(v) = \frac{k}{A}\left(\frac{v}{A}\right)^{k-1} \exp\left(-\left(\frac{v}{A}\right)^{k}\right)$$

where A is the Weibull scale parameter in m/s representing the characteristic wind speed of the distribution. Note that A is proportional to the mean wind speed. In the present studies, this variable is assumed to be 5 m/s that is reasonable for the areas characterized by low wind speed conditions. Variable k characterizes the shape of the Weibull distribution. The value ranges from 1-3, and k = 2 is assumed for the present studies. The Weibull distribution for these parameters is plotted in figure 12. Then, the generated power for the turbine for a year can be calculated based of the Weibull function and the corresponding power curve as

$$E(v) = P(v)f(v)\ [\text{x } 8760\text{h}]$$

and is shown in figure 13. It is shown that the wind turbine power is maximized at a wind speed of 7 m/s throughout the year. The resulting predicted annual energy production (AEP) of the turbine is listed in table 4. It is shown that the energy produced for a year can be increased more than 5.5 times for the curved diffuser case.

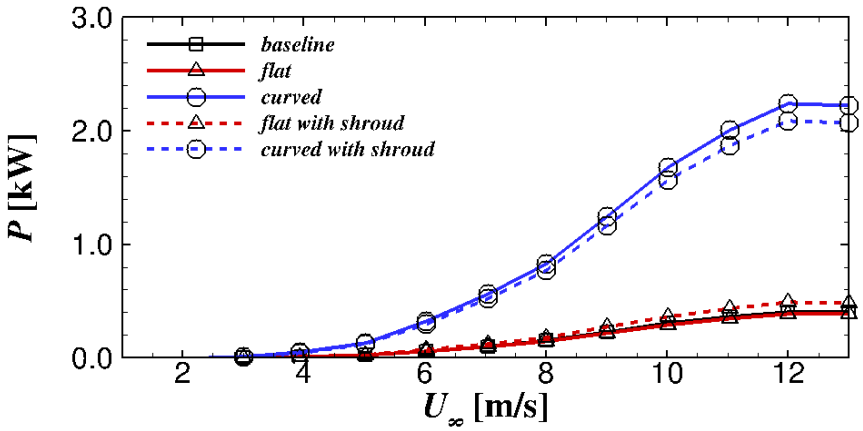

Figure 11. Power curve of the considered wind turbine for various diffusers at x/L = 0.36.

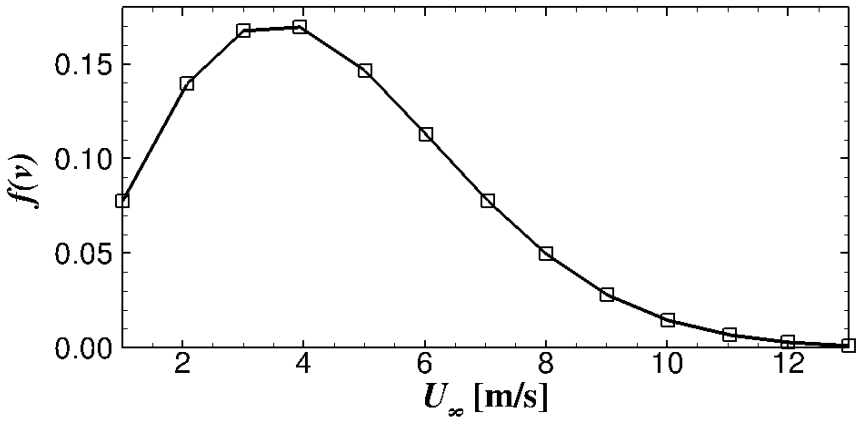

Figure 12. The Weibull distribution of the wind speed for a year.

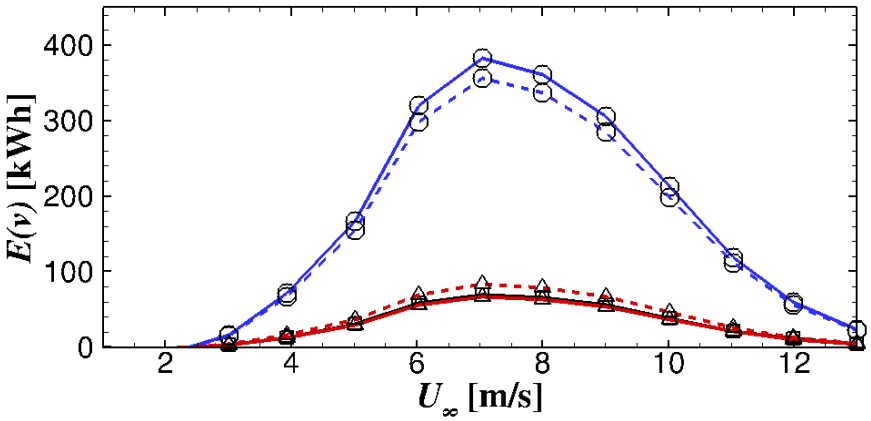

Figure 13. The generated power distribution of the wind turbine for a year at x/L = 0.36.

Table 4. Annual energy production of a turbine for several diffuser types at x/L = 0.36.

Case	AEP [kWh]
Baseline	365.95
Flat	352.72
Curved	2021.73
Flat with shroud	440.68
Curved with shroud	1884.96

4 Conclusions

Numerical simulations have been carried out for flow fields around various diffuser type structures for the application to a shrouded wind turbine. The main conclusions derived from the study are as follows:

- The computational results obtained from the present studies are in good agreement with the corresponding experimental data. Although some discrepancies are observed in the wake area, but the main characteristics of the flow behaviour can be captured.
- The curved diffuser shows the highest improvement of the centreline and average wind velocities along diffuser. The greatest observed increment is 76.99 % at x/L = 0.36 with the maximal average wind velocity of 8.85 m/s. The highest increment of the wind velocity at the diffuser centreline section is 84.18% with the maximal velocity is 9.21 m/s at x/L = 0.285. The difference in increased velocity generated by the curved diffuser compared to flat diffuser is 5.74%.
- It is observed that the improvement of the velocity at the diffuser centreline does not necessarily represent the overall average wind speed. The consideration of the average wind speed remains an important aspect for the energy analysis.
- The flat diffuser with inlet shroud actually generates a higher wind velocity at the entrance section of the diffuser centreline. It is noted, however, that the curved diffuser has a better performance than the flat diffuser, provided that location of the rotor is not at the near entrance but at around $x/L \approx 0.36$.
- Diffusers equipped with the inlet shroud have the smaller average wind velocity at the entrance (inlet diffuser, section x/L = 0) than diffusers without the shroud (section x/L = 0). This fact is in contrary between higher wind velocity result at the diffuser centreline and average wind velocity result. Note that the increased velocity of the diffuser equipped with the shroud actually occurs in the centreline of the diffuser (entrance section, x/L = 0). It shows that the actual wind velocity at the midline diffuser is not capable of representing the overall velocity of each section.
- The flat diffuser with inlet shroud can produce the highest increment of the flow energy production only at inlet diffuser (x/L = 0), while the curved diffuser can produce the best increment of the flow energy production throughout the diffuser.
- The diffuser increases significantly the power generated by the turbine especially at a higher wind speed case. The energy produced for a year can be increased more than 5.5 times for the curved diffuser case.
- From the present studies, it is revealed that the suction effect of the vortex downstream can generate a positive impact on the wind speed quality inside the diffuser. Therefore, flanges can be added on the curved diffuser type structure to generate stronger vortices at the downstream zone aiming to further enhance the suction effect.

5 Acknowledgements

This research leading to these results has received funding from the directorate of research and community service, directorate general of strengthening research and development, ministry of research, technology and higher education of Indonesia.

References

Abe, K.; Ohya, Y.: An investigation of flow fields around flanged diffusers using CFD. *Journal of wind engineering and industrial aerodynamics*, 92, (2004), 315-330.

Bangga, G.: *Three-Dimensional Flow in the Root Region of Wind Turbine Rotors*. kassel university press GmbH, (2018).

Bangga, G.; Hutomo, G.; Wiranegara, R; Sasongko, H.: Numerical study on a single bladed vertical axis wind turbine under dynamic stall. *Journal of Mechanical Science and Technology*, 31(1), (2017a), 261-267.

Bangga, G.; Kusumadewi, T.; Hutomo, G.; Sabila, A.; Syawitri, T.; Setiadi, H.; Faisal, M.; Wiranegara, R.; Hendranata, Y.; Lastomo, D.; Putra, L.: Improving a two-equation eddy-viscosity turbulence model to predict the aerodynamic performance of thick wind turbine airfoils. *Journal of Physics*: Conference Series, 974(1), (2018), 012019.

Bangga, G.; Lutz, T.; Jost, E.; Krämer, E.: CFD studies on rotational augmentation at the inboard sections of a 10 MW wind turbine rotor. *Journal of Renewable and Sustainable Energy*, 9(2), (2017b), 023304.

Bangga, G.; Lutz, T.; Krämer, E.: Root flow characteristics and 3D effects of an isolated wind turbine rotor. *Journal of Mechanical Science and Technology*, 31(8), (2017c), 3839-3844.

Bangga, G.; Sasongko, H.: Dynamic stall prediction of a pitching airfoil using an adjusted two-equation URANS turbulence model. *Journal of Applied Fluid Mechanics*, 10(1), (2017), 1-10.

Bangga, G.; Weihing, P.; Lutz, T.; Krämer, E.: Effect of computational grid on accurate prediction of a wind turbine rotor using delayed detached-eddy simulations. *Journal of Mechanical Science and Technology*, 31(5), (2017d), 2359-2364.

Hu, J.; Wang, W.: Upgrading a shrouded wind turbine with a self adaptive flanged diffuser. *Energies*, 8, (2015), 5319-5337.

Jost, E.; Fischer, A.; Bangga, G.; Lutz, T.; Krämer, E.: 2017. An investigation of unsteady 3-D effects on trailing edge flaps. *Wind Energy Science*, 2(1), (2017), 241-256.

Launder, B. E.; Spalding, D. B.: *Mathematical models of turbulence*, Academic press, (1972).

Menter, F.R.: Two-equation eddy-viscosity turbulence models for engineering applications. *AIAA journal*, 32(8), (1994), 1598-1605.

Ohya, Y.; Karasudani, T.; Sakurai, A.; Abe, K.; Inoue, M.: Development of s shrouded wind turbine with a flanged diffuser. *Journal of wind engineering and industrial aerodynamics*, 96, (2008), 524-539.

Pape, A. L.; and Lecanu, J.: 3D Navier–Stokes computations of a stall regulated wind turbine. *Wind Energy*, 7(4), (2004), 309-324.

Purwanto, D. W.; Nasution, A. M. T.: Interior lengkung diffuser untuk peningkatan performansi diffuser-augmented wind turbine (DAWT), *Prosiding seminar nasional energi terbarukan Indonesia I*, (2010).

Saeidi, D.; Sedaghat, A.; Alamdari, P.; Alemrajabi, A.: Aerodynamic design and economical evaluation of site specific small vertical axis wind turbines. *Applied energy*, 101, (2013), 765-775.

Sørensen, N. N.; Michelsen, J. A.; Schreck, S.: Navier–Stokes predictions of the NREL phase VI rotor in the NASA Ames 80 ft× 120 ft wind tunnel. *Wind Energy*, 5(2-3), (2002), 151-169.

Wang, S.; Ingham, D.B.; Ma, L.; Pourkashanian, M; Tao, Z.: Numerical investigations on dynamic stall of low Reynolds number flow around oscillating airfoils. *Computers & Fluids*, 39(9), (2010), 1529-1541.

Weihing, P.; Letzgus, J.; Bangga, G.; Lutz, T.; Krämer, E.: Hybrid RANS/LES Capabilities of the Flow Solver FLOWer—Application to Flow Around Wind Turbines. *In Symposium on Hybrid RANS-LES Methods Springer, Cham*, (2016), 369-380.

Wilcox, D. C.: *Turbulance modelling for CFD*. DCW Industries, (1993).

Address: [1] Mechanical Engineering Department, State Polytechnic of Ujung Pandang, 90245 Makassar, Indonesia
[2] Mechanical Engineering Department, Institut Teknologi Sepuluh Nopember, 60111 Surabaya, Indonesia
[3] Institute of Aerodynamics and Gas Dynamics, University of Stuttgart, 70569 Stuttgart, Germany
email: [*] klistafani@gmail.com / yiyin_klistafani@poliupg.ac.id,
[†] bangga@iag.uni-stuttgart.de / galih.bangga90@gmail.com